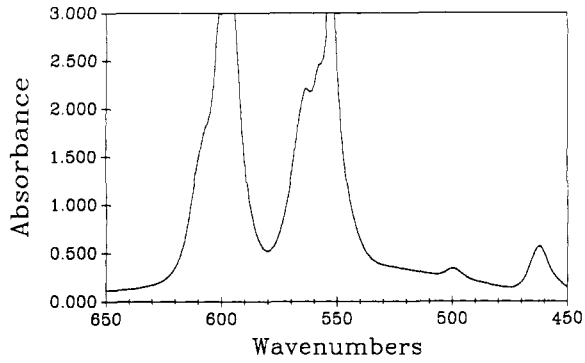

Figure 7. Infrared spectrum of $Cd_2P_2S_6$ fully intercalated with cobaltocene in the region of the PS_3 stretch.

splitting of th PS_3 mode has also been reported for cases where redox does not appear to be the operative mechanism.[5,16] Electronic structure calculations by Whangbo et al.[17] and Mercier et al.[18] on $M_2P_2X_6$ suggest that the acceptor levels in $M_2P_2X_6$ compounds are the divalent metal ions. For the present case, this would result in Cd^0 ($5s^24d^{10}$). Further investigations into the reduced component in this system are ongoing.

Conclusion

Infrared spectra of cobaltocene intercalation compounds of $Cd_2P_2S_6$ are consistent with earlier electron spin resonance studies which concluded that the intercalated cobaltocene is found in both the neutral and cationic state in this compound. Infrared studies on the only other lattice reported to produced mixed oxidation states when intercalated with cobaltocene, SnS_2, were consistent with only one oxidation state in this work. Additional electron spin resonance studies also support the conclusion that the cobaltocene intercalation compound of SnS_2 results in only intercalated cobaltocenium. These results can be interpreted as reflecting the absolute difference in the Fermi level of intercalated $Cd_2P_2S_6$ versus intercalated SnS_2. The time dependence of the infrared spectrum of $Cd_2P_2S_6$ intercalated with cobaltocene suggests that at early reaction times, the cationic form of the cobaltocene is dominant, but that as the reaction proceeds, a significant amount of the intercalated cobaltocene is in the neutral form. The results of this study are consistent with the electronic model proposed by Parkinson et al. to account for mixed valency in charge-transfer intercalation compounds.[10] The lack of neutral cobaltocene intercalated into SnS_2 suggests that in this intercalated material there remains a mismatch between the Fermi level and the redox potential of the cobaltocene in solution. In addition, on the basis of spatially resolved infrared spectra, we have proposed two distinct mechanisms to account for the intercalation and charge transfer processes occurring in the $Cd_2P_2S_6$-cobaltocene system. One involves charge transfer occurring at the edge of the crystal, while the other has charge transfer occurring within the bulk of the crystal.

Acknowledgment. We gratefully acknowledge the support of the National Science Foundation through Grant CHE-9007749 for the electron spin resonance spectrometer used in this work.

(16) Clement, R.; Audiere, J.-P.; Renard, J.-P. *Rev. Chim. Miner.* **1982**, *19*, 560.
(17) Whangbo, M.-H.; Brec, R.; Ouvrard, G.; Rouxel, J. *Inorg. Chem.* **1985**, *24*, 2459.
(18) Mercier, H.; Mathey, Y.; Canadell, E. *Inorg. Chem.* **1987**, *26*, 963.

Chemistry in Polar Intermetallic Compounds. The Interstitial Chemistry of Zr_5Sn_3

Young-Uk Kwon and John D. Corbett*

Department of Chemistry and Ames Laboratory—DOE,[1] Iowa State University, Ames, Iowa 50011

Received July 7, 1992. Revised Manuscript Received August 31, 1992

The formation of stoichiometric Zr_5Sn_3Z derivatives through incorporation of Z within chains of confacial zirconium octahedra in the Zr_5Sn_3 (Mn_5Si_3-type) parent has been studied principally through reactive powder sintering in the range 1000–1350 °C and by X-ray diffraction means. Examples with Z = B, C, N, O, Al, Si, P, S, Cu, Zn, Ga, Ge, Sn, As, and Se have been quantitatively synthesized and characterized as powders. Complications are noted with arc-melting methods and for Z = Fe, Co, Ni where mixed Z–Sn interstitials occur. Single crystal diffraction for Z = C, O, and Ge and Rietveld powder refinement for Ga demonstrate how the host Zr_6 cavities contract or expand to accommodate Z. The $Zr_5Sn_3S_x$ system at 1050 °C is nonstoichiometric over the range $1 > x > \sim 0.5$. Volume trends as a function of Z follow the metallic/covalent radii of Z well.

Introduction

The chemistry of transition metal clusters has recently attracted much attention for its structural diversity and reactivity.[2] Traditionally, stable cluster compounds have been limited to those with discrete structural units in which well-defined electronic requirements are generally understood and satisfied. Metal-rich halides and chalcogenides are such examples.[3-5] Families of these com-

(1) The Ames Laboratory-DOE is operated for the U.S. Department of Energy by Iowa State University under Contract No. W-7405-Eng-82. This research was supported by the Office of the Basic Energy Sciences, Materials Sciences Division.

(2) Lee, S. C.; Holm, R. H. *Angew. Chem., Int. Ed. Engl.* **1990**, *29*, 840.
(3) Simon, A. *Angew. Chem., Int. Ed. Engl.* **1988**, *27*, 159.
(4) Chevrel, R.; Sergent, M. In *Crystal Chemistry and Properties of Materials in Quasi-One-Dimensional Structures*; Rouxel, J., Ed.; Reidel: Dordrecht, 1986; p 315.

0897-4756/92/2804-1348$03.00/0

pounds usually achieve 3D structures via intercluster bridging with exo nonmetal atoms. Halides of the earlier transition metals achieve a particularly rich cluster chemistry through the encapsulation of diverse interstitial elements.[5] Condensed cluster products are also obtained in compounds with lower nonmetal:metal ratios, generally through edge sharing of the octahedral metal clusters of the earlier elements.

Cluster structures are also found in a class of compounds we have termed "polar intermetallics", combinations of the pre- or early transition elements with main-group metals or metalloids from the aluminum through the phosphorus families. Their structures are generally more condensed because of the smaller proportions of main group "anions". A prime example is the large number of A_5B_3 compositions in the Mn_5Si_3 structural family in which confacial octahedra of the transition (A) element form quasi-infinite chains. These phases are, in contrast to many traditional cluster examples, usually metallic in character since the number of valence electrons from the A element well exceeds the requirements of the isolated B elements therein. Several examples of this structure have recently been found to bind quantitative amounts of a variety of interstitial elements within the octahedral (antiprismatic) metal chains, just like in some more conventional clusters, although the products are generally not electronically precise.[6-8]

The results of such a recent study of the interstitial products formed by the Zr_5Sb_3 host provide some useful background.[8] First, the 15 different interstitial elements (Z) that may be incorporated in stoichiometric phases Zr_5Sb_3Z by and large consist of main-group elements, excepting the halogens and noble gases, plus a few late transition elements. This large structural flexibility and electronic variability has not been observed in traditional (transition metal) cluster compounds, although rare-earth-metal iodides approach this for platinum metal Z.[9] Second, this study showed that several previously supposed interstitial examples Zr_5Sb_3Z had, in fact, been mistakenly interpreted. Many experimental problems can arise in these cases, not just from impurities but also from the need for quality syntheses at high temperatures. For example, arc melting can be particularly troublesome as it often affords phases that are substoichiometric or contain mixed interstitials. Therefore, scrupulous examinations of synthetic conditions with respect to equilibria and impurities, as often reflected in product lattice parameters, are needed in order to ensure successful syntheses. The alternate formation of the series of compounds $Zr_5B_{2+x}T_{1-x}$ (B = Sn, Sb; T = Fe, Co, Ni, Ru, Rh) in substituted W_5Si_3-type structures has also demonstrated that even slight deviations from Zr_5B_3Z compositions may result in drastic changes.[10]

In the present paper, we report the analogous interstitial chemistry of Zr_5Sn_3, a host in the same structure type but somewhat less electron-rich (5·4 − 3·4 = 8 e^- vs 5·4 − 3·3 = 11 in Zr_5Sb_3). This and slight variations of crystallographic parameters in fact produce only small effects on the interstitial chemistry. We have previously studied the Zr–Sn binary system, particularly Zr_5Sn_3 and Zr_5Sn_4 where a fourth tin occupies the interstitial site in the former phase.[11] The eventual merging of their phase fields at higher temperature and the congruent melting of an intermediate composition $\sim Zr_5Sn_{3.3}$ further emphasize the complications that may pertain to arc-melting routes. These properties and the interstitial chemistry are also relevant to Zircaloy cladding materials.[10-12]

Experimental Section

Materials. Reactor grade zirconium was used in all reactions. This, its cleaning and the generation of powdered Zr were as described previously.[11] Tin granules (Baker's Analyzed: 99.99%) did not show any dross upon fusion and were employed as received. Sources of other reagents were: B (99.5%) and Co (99.9 + %), Aesar; ZrC and ZrN, Cerac; Al (high purity), United Mineral & Chemical; Ti (crystal bar) Ames Lab.; P (5-9's) and As (6-9's), Aldrich; S (5-9's), Alfa Products; Cr and Mn (99.9%), A. D. Mackay; Fe (99.9%), Plastic Metals; Ni (reagent) Matheson Coleman & Bell; Cu (4-9's), J. T. Baker; Zn (4-9's), Fischer Scientific; Ga (4-9's), Si and Ge (5-9's, zone refined) and ZrO_2, Johnson Matthey; Se (5-9's), American Smelting & Refining; Ag (reagent), G. F. Smith Chem. Co.; Cd (5-9's), Cominco Products. The Zn was sublimed and the oxide surfaces were scraped off Al, Ga, and Cd before use.

Syntheses. All powdered or ground reagents were prepared and handled only in a glovebox. Reactive sintering of mixtures of Zr, $ZrSn_2$ and ZrZ_x powders that had first been pressed into pellets was the major technique for Zr_5Sn_3Z syntheses, the $ZrSn_2$ and ZrZ_x being selected for their ease of grinding. The reagent $ZrSn_2$ was synthesized from stoichiometric amounts of Zr powder and Sn in a sealed Ta tube at 800–1000 °C. ZrZ_x's were obtained similarly when possible. When the mobilities of Z elements were considered, or found, to be too low to form desired compounds by this method, arc-melting reactions were utilized, and the ground product used in the same way. The forms of ZrZ_x were ZrC, ZrN, ZrO_2 as received, ZrAg, ZrS_2, $ZrGa_3$, $ZrGe_2$, ZrAs, $ZrSe_2$ from powder reactions as for $ZrSn_2$ (above), and $ZrAl_2$, $ZrFe_2$, $ZrCo_2$, ZrNi and Zr_3Cu_2 from arc-melting. All binary reagents so prepared were examined by Guinier powder diffraction to verify phase purity, lattice parameters, and structure type. B and Si were used as the elements.

The volatile elements P, S, As, and Se would attack the Ta container at temperature, and they were obviously not suitable for prior arc-melting reactions. Therefore, stoichiometric mixtures of Zr_5Sn_3 and these Z as powders were first reacted in evacuated silica tubes at 500–600 °C for ~6 days to produce intimate mixtures of products, and these were then powdered and used for sintering reactions. In these cases, Zr_5Sn_3 was synthesized by sintering Zr and $ZrSn_2$ powders at 1000 °C lest any self-interstitial or impurity from arc-melting interfere or upset the material balances.

Pressed pellets were sealed in Ta tubes with 0.08-mm Mo liners, and these were in turn encapsulated in baked and evacuated silica tubes for sintering below 1150 °C. For reactions at higher temperature, the sealed Ta containers were heated under a dynamic vacuum (10^{-6} Torr) in a high-temperature furnace described before.[10,11]

Vapor-phase transport reactions were attempted for some Zr_5Sn_3Z systems within long Ta tubes (>7 cm) in two-zone furnaces and with $ZrCl_4$ as the transport agent. The chloride proved to be better than other ZrX_4 for transport and crystal growth.

Arc-melting reactions sometimes produced rodlike crystals during cooling. Details of the reaction conditions and some problems associated with this method of crystal growth are elaborated elsewhere.[8,10,11]

X-ray Studies. Guinier powder diffraction techniques were employed as the primary means of examination of all synthesized samples. Lattice parameters were obtained at room temperature by least-squares refinement of indexed line positions calibrated by an internal silicon standard (NIST). The relative intensities

(5) Corbett, J. D. In *Modern Perspectives in Inorganic Crystal Chemistry*; Parthé, E., Ed.; NATO ASI Series C, Klewer Academic Publishers: Dordrecht, in press.
(6) Hurng, W.-M.; Corbett, J. D. *Chem. Mater.* **1989**, *1*, 311.
(7) Corbett, J. D.; Garcia, E.; Kwon, Y.-U.; Guloy, A. *Pure Appl. Chem.* **1990**, *62*, 103.
(8) Garcia, E.; Corbett, J. D. *Inorg. Chem.* **1990**, *29*, 3274.
(9) Rogel, F.; Zhang, J.; Payne, M. W.; Corbett, J. D. *Adv. Chem. Ser.* **1990**, *226*, 369.
(10) Kwon, Y.-U.; Sevov, S. C.; Corbett, J. D. *Chem. Mater.* **1990**, *2*, 550.
(11) Kwon, Y.-U.; Corbett, J. D. *Chem. Mater.* **1990**, *2*, 27.
(12) Kwon, Y.-U.; Corbett, J. D. *Chem. Mater.* **1992**, *4*, 187.

Table I. Single-Crystal Collection and Refinement Data for Zr_5Sn_3Z (Z = C, O, Ge)

	Z		
Z	C	O	Ge
Space group, Z	$P6_3/mcm$ (no. 193), 2		
a,[a] Å	8.4268 (9)	8.4256 (8)	8.6414 (9)
c, Å	5.8001 (8)	5.763 (1)	5.866 (1)
μ(Mo Kα), cm^{-1}	173	173	201
indep reflns ($I > 3\sigma(I)$)	139	163	130
variables	13	13	14
R, R_w[b]	2.6, 2.6	1.8, 2.3	5.5, 5.5

[a] Guinier data. [b] $R = \sum||F_o| - |F_c||/\Sigma|F_o|$; $R_w = [\sum w(|F_o| - |F_c|)^2/\sum w(F_o)^2]^{1/2}$; $w = [\sigma(F)]^{-2}$.

in the powder patterns were also utilized to estimate levels of impurities, if any, in the products. The detection limit with this technique can be as low as 1%, 3–4% more typically, when all phases are crystalline.

Single crystals were utilized for X-ray structural refinements in some cases. DATEX, CAD 4, or Rigaku AFC6R diffractometers and their accompanying CHES,[13] SDP,[14] or TEXSAN[15] packages, respectively, were used to collect ($2\theta \leq 55°$), process, and refine the absorption-corrected data. The collected data, sometimes supported by oscillation and zero-layer Weissenberg photographic studies, all indicated systematic extinctions and averaging appropriate to the $P6_3/mcm$ space group of Mn_5Si_3, and the structures were refined accordingly. Occupancies, anisotropic thermal parameters and secondary extinction parameters were also refined. Some crystallographic data are given in Table I.

A powdered gallium product from a sintering reaction was also examined by Rietveld methods.[16] Intensity data were obtained on a Rigaku θ–θ diffractiometer[17] with Cu Kα radiation over a $15° \leq 2\theta \leq 90°$ range in 0.02° intervals. An Mn_5Si_3-type structure was assumed for the refinement. A Pearson-VII peak profile function and 3- or 4-polynominal background parameters were utilized. Convergence at $R = 8.11\%$, $R_w = 10.78\%$ for the profile and $R_I = 1.43$, $R_F = 0.72\%$ for intensities were obtained.

SEM/EDX Studies. A JEOL JSM-840 electron microscope was used to examine the more complex Fe-containing samples for the phases present and their compositions. Samples were dry polished with a series of sandpapers and finally with ash. $ZrFe_2$ and Zr_5Sn_3 samples prepared in the same manner were utilized as standards.

Results and Discussion

Assessment of the synthetic schemes and results for interstitial compounds of Zr_5Sn_3 requires prior knowledge of its Mn_5Si_3-type structure.[18] Figure 1 shows the hexagonal structure projected along and perpendicular to c̄. Two zirconium chains run in the c direction, those built of confacial trigonal antiprisms of Zr2 (Mn2) along 0, 0, z and linear chains of Zr1 (Mn1) at $^1/_3$, $^2/_3$, z, etc., with $z = 0, ^1/_2$. These metal chains are surrounded by a single type of Sn (Si) atoms that (a) bridge edges of the shared faces of the trigonal antiprisms of Zr2, (b) are exo to Zr2 in neighboring chains, and (c) form distorted confacial trigonal antiprisms about Zr1 in the linear chains. The centers of the $(Zr2)_6$ antiprisms in the confacial chains are vacant in the host structure, but these can in many cases be stuffed with diverse interstitial elements (Z) to form Zr_5Sn_3Z compounds that show small parametric changes

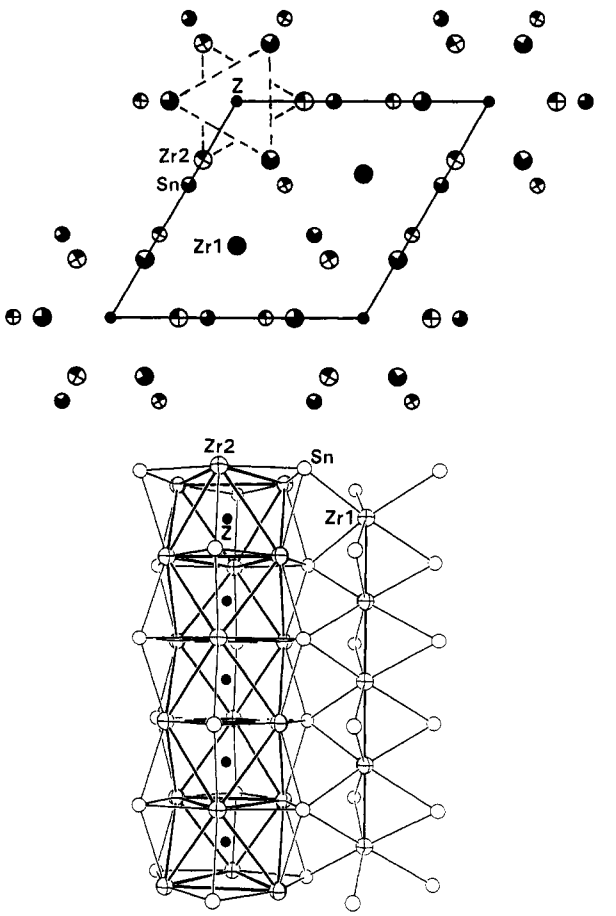

Figure 1. Stuffed Mn_5Si_3-type (or Ti_5Ga_4) structure of Zr_5Sn_3Z. Top: [001] projection with large circles Zr, medium circles Sn, small circles interstitial Z. The atoms are shaded according to their height in z: solid ones are at 0 and $^1/_2$. One confacial Zr2 chain is outlined. Bottom: A portion of a [110] section showing the confacial trigonal antiprismatic chain of Zr2 edge-bridged by Sn (left), the linear chain of Zr1 atoms (right), and the shared Sn. (Zirconium is larger and crossed, tin medium and open, Z small solid circles.)

but no other significant alterations in the structure.

Syntheses. We earlier established the existence of stoichiometric Zr_5Sn_3 and its self-interstitial Zr_5Sn_4 in which the fourth extra tin occupies the interstitial site (Ti_5Ga_4 type[19]).[11] These are line phases at ~1100 °C, but the compositions broaden toward each other at higher temperatures and coalesce into a single solid solution Zr_5Sn_{3+x}, $0 \leq x \leq 1$, that terminates at a congruent melting point at x ~0.3 and ~1990 °C. Synthesis via arc-melting reactions, a very high-temperature method by nature, always produces partial tin interstitials and, frequently, considerable sample inhomogeneity on cooling because of the nature of the liquid–solid relationships. The ternary interstitial phases reported here were all synthesized or annealed below 1300 °C to avoid these and related problems, while arc-melting was the least utilized technique. Earlier studies of Zr_5Sb_3Z systems elaborated the problems of arc melting as a synthetic route.[8]

Several criteria were used in determining whether a given reaction product and its lattice parameters represented a stoichiometric equilibrium phase. Some structure refinements provided firsthand evidence. A quantitative yield of a single phase without any detectable impurities (by X-ray) and the reproducibility of the results with different conditions were the most crucial conditions to

(13) For detailed references, see: Hwu, S.-J.; Corbett, J. D.; Poeppelmeier, K. R. *J. Solid State Chem.* **1985**, *57*, 43.
(14) SDP User's Guide, Enraf-Nonius, Delft, Holland and B. A. Frenz & Associate, Inc. College Station, TX, 1988.
(15) TEXSAN: Single Crystal Structure Analysis Software, Version 5.0, Molecular Structure Corporation, The Woodlands, TX, 1989.
(16) Rietveld, H. M. *J. Appl. Crystallogr.* **1969**, *2*, 65.
(17) Described in: Kim, S.-J.; Nguyen, T.-H.; Franzen, H. F. *J. Solid-State Chem.* **1987**, *70*, 88.
(18) Aronsson, B. *Acta Chem. Scand.* **1960**, *14*, 956.
(19) Pötzschke, M.; Schubert, K. *Z. Metallkd.* **1962**, *52*, 474.

Table II. Reaction Conditions for Zr_5Sn_3Z Syntheses

Z	reagents	method[a]	T (°C)	time, days	other phases (%)
B	Zr, $ZrSn_2$, B	S	1300, 1350	3,5	ZrB_2, ZrO_2 (<5)
C	Zr_5Sn_3, C	S	1000	10	Zr_2SnC
	Zr, $ZrSn_2$, ZrC	S	1350	5	
N	Zr, $ZrSn_2$, ZrN	S	1300, 1350	3,5	ZrN(<5)
O	Zr, $ZrSn_2$, ZrO_2	S	1350	5	impurities
	Zr, $ZrSn_2$, ZrO_2	V	900/850		(Zr, Zr_5Sn_4)
Al	Zr, Sn, Al	AN	1000	10	
Si	Zr, $ZrSn_2$, Si	S	1000	6	
P	Zr_5Sn_3, P	R	500	6	
		S	1100	13	ZrP (<5)
S	Zr_5Sn_3, S	R	500	6	
		S	1100	13	
Cu	Zr, $ZrSn_2$, Zr_3Cu_2	S	1000	10	
Zn	Zr_5Sn_3, Zn (1:5)	G	1000	9	
Ga	Zr, $ZrSn_2$, $ZrGa_3$	S	1000	7	
Ge	Zr, $ZrSn_2$, $ZrGe_2$	S	1350	5	
As	Zr_5Sn_3, As	R	500	6	
		S	1100	13	ZrAs (<5)
Se	Zr_5Sn_3, Se	R	500	6	
		S	1000	14	
	Zr, $ZrSn_2$, $ZrSe_2$	S	1000	14	
$Fe_{1/3}Sn_{1/3}$		AN	1300	3	
$Co_{1/3}Sn_{1/3}$		AM			
$Ni_{1/3}Sn_{1/3}$		AM			

[a] S, sinter; V, vapor transport with $ZrCl_4$; AN, anneal after arc-melt; R, prereaction in silica; G, zinc vapor; AM, arc-melt.

be met. Complimentary SEM/EDX studies in this and other systems (Zr_5Sb_3Z, La_5Ge_3Z especially) have supported the validity of these criteria. Lattice parameters that were distinctive from those of binary Zr_5Sn_3 and Zr_5Sn_4 phases were also important indications of the interstitial event. Sharper diffraction lines and greater divergence of the lattice parameters from those of the parent Zr_5Sn_3 generally accompany improved crystallinity and order.

Reaction conditions for successful syntheses are listed in Table II, and the lattice parameters are given in Table III, including reference values for Zr_5Sn_3 and Zr_5Sn_4. The following paragraphs provide separate particulars and details about each system when these are not clear from the tables.

Boron. An initial reaction at 1300 °C yielded the apparent interstitial phase plus ZrB_2 and ZrO_2, so the product was ground, repelleted, and sintered further at 1350 °C for 5 days. This resulted in the same lattice parameters for the hexagonal phase and much reduced proportions of ZrB_2 and ZrO_2 (<5% total). Similar problems have been encountered in the Zr_5Sb_3B system, and the source of oxygen may be the boron. The stoichiometry is not ensured when impurities are present, but the unchanged lattice parameters with different impurity levels imply that the interstitial phase is close to stoichiometric.

Carbon. A sintering reaction at 1000 °C with Zr_5Sn_3 and C powders gave mainly Zr_2SnC plus unreacted Zr_5Sn_3, the latter having dimensions very close to those of the binary. The former is typically synthesized at 800 °C. A higher temperature, 1500 °C for 4 h, gave the interstitial phase (a = 8.4298 (8), c = 5.799 (1) Å) as the major product. A single phase product (a = 8.4238 (5), c = 5.8011 (7) Å) was obtained from a sintering reaction at 1350 °C for 5 days. The two are averaged in Table III. Arc-melting of the 1500 °C product produced single crystals with close to the stoichiometric composition (see Crystal Chemistry below).

Nitrogen. The synthesis of this phase paralleled that of the boride, sintering at 1300 °C followed by additional sintering at 1350 °C after grinding and repelleting. The amount of unreacted impurity ZrN was successively reduced from 10% to <5% even though the respective lattice parameters, a = 8.4030 (7), c = 5.7695 (7) Å and a = 8.4050 (8), c = 5.7700 (8) Å, were virtually identical.

Table III. Lattice Parameters of Interstitial Compounds Zr_5Sn_3Z[a]

Z	a (Å)	c (Å)	V (Å^3)	c/a
B	8.4936 (4)	5.8029 (5)	362.54 (5)	0.683
C[b]	8.4268 (9)	5.8001 (8)	356.69 (9)[c]	0.688
N	8.4040 (8)	5.7698 (8)	352.91 (8)[c]	0.687
O[b]	8.4256 (8)	5.763 (1)	354.31 (9)[c]	0.684
Al	8.655 (1)	5.871 (1)	380.9 (1)	0.678
Si	8.6072 (9)	5.844 (1)	374.9 (1)	0.679
P	8.5449 (5)	5.9171 (7)	374.16 (6)	0.692
S	8.5065 (5)	5.9646 (6)	373.78 (6)[c]	0.701
Cu	8.6249 (7)	5.877 (1)	378.61 (9)	0.681
Zn	8.6325 (7)	5.877 (1)	379.28 (9)	0.681
Ga[b]	8.6599 (6)	5.8794 (8)	381.85 (7)	0.679
Ge[b]	8.6414 (9)	5.866 (1)	379.4 (1)[c]	0.679
As	8.6037 (6)	5.9200 (9)	379.51 (8)[c]	0.688
Se	8.5584 (5)	5.9515 (6)	377.52 (6)[c]	0.695
$Fe_{1/3}Sn_{1/3}$	8.6063 (5)	5.8639 (7)	376.14 (6)	0.681
$Co_{1/3}Sn_{1/3}$	8.5934 (7)	5.861 (1)	374.82 (9)	0.682
$Ni_{1/3}Sn_{1/3}$	8.5812 (6)	5.8577 (8)	373.55 (7)	0.683
$Sn_{0.10}$	8.4802 (5)	5.7950 (7)	360.91 (6)	0.683
Zr_5Sn_3[d]	8.4560 (7)	5.779 (1)	357.86 (9)	0.683
Zr_5Sn_4[d]	8.7656 (7)	5.937 (1)	395.06 (9)	0.677

[a] Stuffed Mn_5Si_3-type (space group $P6_3/mcm$). From Guinier powder data with λ = 1.540 56 Å. Synthetic conditions in Table II. [b] Structure refined. [c] Average of data for more than one sample. [d] Reference 11.

Oxygen. A sintering reaction at 1350 °C for 5 days yielded an interstitial phase (a = 8.4257 (7), c = 5.7611 (9) Å) along with many weak impurity lines. A product with a larger unit cell (a = 8.4333 (5), c = 5.7661 (5) Å) plus ~5% unreacted ZrO_2 was obtained from the same reactants at 1650 °C for 4 h. The latter are comparable to those from an arc-melted product (a = 8.4361 (6), c = 5.7643 (7) Å) for which a single-crystal composition was refined (below). Since second period interstitials reduce the lattice parameters of the host, the a parameter especially in the last suggests some oxygen substoichiometry.

Unlike ternaries with other second-period elements, the oxygen product could also be synthesized through a mineralization reaction with $ZrCl_4$ at 900 °C. No material transfer to the cooler zone occurred, but the product had parameters of an oxide phase (a = 8.4255 (8), c = 5.765 (1) Å).

Some indirect evidence for a substoichiometric oxide was obtained for $Zr_5Sn_3O_x$ compositions, x = 0.1 and 0.5, that were arc-melted, ground, and sintered at 1100 °C for 7 days. The first showed a single phase (a = 8.4540 (7), c = 5.7700 (9) Å) only slightly smaller than the empty host, while an apparent oxide (a = 8.4338 (6), c = 5.7608 (8) Å) phase plus many unidentified lines were obtained for $x \sim 0.5$.

Aluminum. Arc-melting of the elements repeatedly gave an interstitial phase with much smaller parameters plus Zr_4Al_3 (~15%), but these produced a single hexagonal product on annealing. Structural refinement of a single crystal from an arc-melting reaction (below) showed large deviations from stoichiometry. Repeated powder sintering reactions at 1100 °C never yielded a single-phase product, rather two Mn_5Si_3-like phases. The overall behavior resembles that of the "Zr_5Sn_3Fe" system (see below).

Phosphorus. Prereaction of stoichiometric amounts of Zr_5Sn_3 and P powders gave a product that could be sintered at 1100 °C without attack of the container. The amount of ZrP in the final product was estimated to be less than 5%.

Sulfur. A good product was obtained under the same condition as for phosphorus, and a quantitative yield with lattice constants only ~0.002 Å larger was also obtained by sintering of Zr, $ZrSn_2$, and ZrS_2 for 5 days at 1350 °C. Table III lists the average.

The sulfur system was also studied regarding substoichiometric products $Zr_5Sn_3S_x$. A prereacted sample of the Zr_5Sn_3S composition was pelleted with appropriate amounts of Zr_5Sn_3 to furnish $x = {}^1/_3$, ${}^1/_2$, and ${}^2/_3$ samples, and these sintered at 1050 °C for 7 days. Only the last yielded a single sulfide phase while the first two showed mixtures of the ternary sulfide with ~20 and <5%, respectively, of a Zr_5Sn_3-like phase. The lattice parameters are discussed in a later section.

Copper. A quantitative synthesis was achieved through reactive sintering. The lattice parameters reported earlier by Rieger et al.[20] from a Zr_5Sn_3Cu synthesis in fused silica, probably at 1100 °C for 0.5 day (a = 8.75, c = 5.90 Å), are much larger than those found here with Cu as well as for the neighboring Zn, Ga, Ge derivatives. They are in fact quite a bit closer to those for Zr_5Sn_4 (a = 8.7418 (7), c = 5.926 (1) Å), but the effects of other probable impurities cannot be judged.

Zinc. A representative zinc example was obtained by reacting Zr_5Sn_3 powder with excess zinc vapor in tantalum.

Gallium. A single-phase sample was synthesized by reactive sintering, as indicated. This sample was also analyzed with a Rietveld X-ray refinement and found to be stoichiometric (see below). As in the aluminum case, many rod crystals were produced during the rapid cooling that follows arc-melting reactions. However, these have much smaller lattice parameters, and refinement of the structure of one of these crystals (below) showed that the interstitial site was not fully occupied.

Germanium. Sintering reactions at 1100 and 1350 °C both yielded single-phase products to X-rays with identical c parameters and a parameters that increased with reaction temperature, but only by 3.7σ. Their average appears in Table III. Very thin needle crystals were found on the surface of a pellet sintered at 1100 °C. A single-crystal refinement of one (below) showed it to be stoichiometric Zr_5Sn_3Ge although the standard deviations were somewhat high. The lattice parameters of this single crystal were also close to those of the sintered products.

Selenium. As with the sulfur analogue, two different methods (Table II) produced the same lattice parameters within 3.2 and 4.6σ. The average is reported.

Iron. This system exhibits some appreciable complications. Arc-melting reactions with the ideal 5:3:1 composition yielded an hexagonal interstitial phase plus a very faint but consistent extra line in the powder patterns. The lattice parameters (typically a = 8.599 (2), c = 5.853 (1) Å) fluctuated severely with temperature, time, starting materials, and method, but the persistent extra line could be explained in terms of cubic $ZrFe_2$ wth some tin substitution. Annealing the as-cast buttons at 1000–1150 °C always caused the lines of the interstitial phase to become very diffuse. Interestingly, sintering reactions of Zr, $ZrSn_2$, and $ZrFe_2$ in this temperature region gave completely different powder patterns, typically of three phases, two Mn_5Si_3-types and $ZrFe_2$, over a variety of reaction times. The lattice parameters of the pair of Mn_5Si_3-type phases changed with the starting composition. A Zr_5Sn_3Fe sample gave a = 8.4219 (5), c = 5.7632 (6) Å and a = 8.671 (1), c = 5.884 (1) Å, and $Zr_5Sn_3Fe_{0.75}$, a = 8.412 (2), c = 5.788 (2), Å and a = 8.7231 (7), c 5.912 (1) Å. The first in each sample is smaller than that of the binary host or any stuffed version except with small nonmetals, and the dimensions of the latter approach those of Zr_5Sn_4. Substitution of other transition metals at the Mn positions are known in other Mn_5Si_3-type compounds, and the smaller phase could be understood as that from iron substitution for zirconium, probably without interstitial atoms, while the latter might contain a mixed tin–iron interstitial Zr_5Sn_3X that would result from the stoichiometry imbalance produced by $ZrFe_2$ precipitation.

Interestingly, apparently singe-phase products with well-defined lines could be obtained from annealing or sintering reactions run at 1300 °C or above. The lattice parameters of these samples agreed reasonably well with those from as-cast samples. However, SEM/EDX studies on samples from these that were single phase by powder pattern showed that domains of the major phase (10–100 μm) varied in composition from $Zr_5Sn_{3.64}Fe_{0.32}$ to about $Zr_5Sn_{3.29}Fe_{0.49}$ (uncertainties 0.03–0.05). A minor phase (probably $ZrFe_2$-based) at the domain boundaries ranged from about $ZrSn_{0.75}Fe_{1.08}$ to $Zr_5Sn_{0.04}Fe_{1.65}$. Although the accuracy of the method and the very small domains require reservations regarding the latter compositions, it was obvious that the impurity phase was iron-rich.

The implication of the EDX results is that there is a solid solution of $Zr_5Sn_3(Sn_xFe_{1-x})$ over some range above 1300 °C. Therefore, compositions with $x = {}^1/_3$, ${}^1/_2$, ${}^2/_3$, and $Zr_5Sn_3(Sn_{1/3}Fe_{1/3})$ were arc-melted and annealed at 1300 °C for 8 days. All but the first $Zr_5Sn_{3.33}Fe_{0.67}$ sample were single phase to both powder patterns and SEM, and the impurity in this was the same as before.

The powder patterns of the above as-cast samples showed broad bands reminiscent of the behavior of the Zr_5Sn_3–Zr_5Sn_4 system[11] except that $Zr_5Sn_3(Sn_{1/3}Fe_{1/3})$ gave a sharp powder pattern of a single hexagonal phase. We tentatively conclude that the congruently melting composition is close to $Zr_5Sn_3(Sn_{1/3}Fe_{1/3})$ and, therefore, as-casts from "Zr_5Sn_3Fe" compositions contained ~$Zr_5Sn_{3.3}Fe_{0.3}$ with the remaining Zr and Fe as $ZrFe_2$(Sn). Even though the lattice parameters fluctuated with composition, the average dimensions of the as-cast product (a = 8.599 (2), c = 5.853 (1) Å) are close to those of $Zr_5Sn_3(Sn_{1/3}Fe_{1/3})$ made at 1300 °C (a = 8.6063 (5), c = 5.8639 (7) Å).

The low-temperature instability of the mixed interstitial phase implied by the above sintering and annealing results was doubly confirmed by sintering a ground $Zr_5Sn_3(Sn_{1/3}Fe_{1/3})$ as-cast at 1000 °C. This produced a powder pattern similar to that obtained after reactive sintering (above); two Mn_5Si_3-type phases, one with smaller and the other with larger lattice constants than Zr_5Sn_3.

On the basis of these observations, we propose a ternary analogue of the Zr_5Sn_3–Zr_5Sn_4 system,[11] a solid solution of $Zr_5Sn_3(Sn_xFe_{1-x})$ above 1300 °C from x = 1 to about ${}^1/_3$, the range narrowing as the temperature rises to the congruent composition near $Zr_5Sn_3(Sn_{1/3}Fe_{1/3})$. Near 1000 °C there are only two line phases, Zr_5Sn_3 and Zr_5Sn_4, with some partial substitution of Fe in the former. The iron content in the analogous Zr_5Sb_3 host is limited to a composition near $Zr_5Sb_{3.3}Fe_{0.3}$. Less tin in the present system affords $Zr_5Sn_{2+x}Fe_{1-x}$ phases that are related to W_5Si_3 with some iron substitution for tin.[10]

Cobalt. The overall behavior is virtually identical to that of iron compound. Arc-melting of Zr_5Sn_3Co (a = 8.585 (2), c = 5.845 (1) Å) and $Zr_5Sn_3(Sn_{1/3}Co_{1/3})$ (Table III) compositions gave comparable lattice parameters. The former contained $ZrCo_2$ and the latter was impurity-free.

(20) Rieger, W.; Nowotny, H.; Benesovsky, F. *Monatsh. Chem.* **1965**, *96*, 232.

Nickel. Almost everything in this system parallels that of cobalt. The impurity phase at the Zr_5Sn_3Ni composition is $ZrNi_3$.

Titanium to Manganese. Various synthetic approaches for these phases all showed that no stuffed hexagonal phase is formed. Instead, the zirconium atoms in the host lattice are apparently substituted by the smaller, early 3d elements. It is remarkable that even phases with mixed interstitials as seen in the Zr_5Sn_3–Fe system are not formed. An arc-melted $Zr_5Sn_3(Sn_{1/3}Cr_{1/3})$ composition contained elemental Cr and gave lattice parameters (a = 8.5535 (8), c = 5.8522 (9) Å) that were unmistakably smaller than those from the corresponding Fe–Ni systems, appearing rather to be those of $Zr_5Sn_{3.3}$ as-casts.

Silver. Fluctuating lattice parameters typify this system even for the same starting compositions. Mixed interstitials are assumed.

Cadmium. Reactions analogous to those for zinc proved only that cadmium cannot be incorporated interstitially to a significant extent.

Others. Reactions with Te and Sb did not produce significant changes in dimensions. Substitution of lattice tin by these might be expected to give problems. Neither chloride or fluoride could be incorporated.

Partial Tin Interstitial. To grow single crystals of Zr_5Sn_3, an arc-melted button with this composition was annealed at 1800 °C for 2 h in a capped Mo crucible. The reason for the high temperature was to overcome the gross compositional inhomogeneities known for such as-cast products.[11] A single crystal was obtained from the product which now gave only sharp lines in its powder pattern. Both the structure refinement and the larger lattice parameters indicated that the phase thus obtained contained about 10% interstitial tin (below).

Crystal Chemistry. Table IV summarizes the single-crystal structural refinement results. Those with C, O, Ga, and Ge interstitials were found to be substantially stoichiometric, while Al and Ga analogues from arc-melting reactions were not, giving 112 (2) and 84.0 (5)% interstitial occupancies, respectively, when the intended element was refined. As discussed previously,[8] we understand these as mixed interstitials with tin or vacancies (or both); the cavity (Zr2–Ga) dimension in the latter is consistent with vacancies, being 0.05 Å less than in the fully occupied (Rietveld) result.

Distances for the better-defined compositions and those extrapolated for the empty host are given in Table V. The most obvious and interesting changes in distances are those for Zr2–Z with Z. The C and O contract the cavity radius by 0.08 Å from that in the empty host, while the edges of the Zr2 trigonal antiprism decrease therewith by 0.10–0.12 Å. The Zr2–Sn distances simultaneously increase by about 0.04 Å on average while the tin moves somewhat closer to Zr1. The Zr2–C (2.459 Å) and Zr2–O (2.456 Å) distances in these crystals are strikingly larger than those of the binary and very different ZrC (2.348 Å[22]) and $ZrO_{0.7}$ (2.292 Å[23]), respectively, presumably in part because the large tin atoms dominate the structure and provide a matrix effect that limits the collapse of the zirconium antiprisms. A remarkable, opposite deviation, d(Zr–C) = 2.287 Å, is found within Zr_6C cluster units when these are enclosed in halide, e.g., in $Rb_4Zr_6(C)Cl_{18}$.[24]

Table IV. Refined Parameters for Zr_5Sn_3Z (Z = C, O, Al, Ga, Ge)[a]

atom	x	B_{iso}	occ
		C	
Sn	0.6034 (1)	0.49 (3)	1.002 (3)
Zr1	$^1/_3$	0.39 (4)	1
Zr2	0.2357 (2)	0.87 (5)	1.013 (3)
Z	0	0.8 (4)	1.08 (6)
		O	
Sn	0.60260 (6)	0.69 (3)	1.003 (3)
Zr1	$^1/_3$	0.53 (3)	1.000 (5)
Zr2	0.2359 (1)	0.81 (4)	1
Z	0	0.3 (2)	0.92 (3)
		Ge	
Sn	0.6126 (3)	0.9 (1)	1.02 (2)
Zr1	$^1/_3$	0.6 (1)	1
Zr2	0.2724 (4)	1.6 (2)	1.07 (3)
Z	0	0.4 (2)	0.94 (6)
		Ga[b]	
Sn	0.6117 (5)	1.54 (9)	1
Zr1	$^1/_3$	1.2 (2)	0.99 (2)
Zr2	0.2674 (5)	1.4 (1)	1.00 (1)
Z	0	1.3 (4)	0.99 (3)
		Al[c]	
Sn	0.6127 (1)	0.46 (2)	0.996 (4)
Zr1	$^1/_3$	0.76 (3)	1
Zr2	0.2657 (2)	0.26 (2)	0.993 (6)
Z	0	0.34 (7)	1.12 (2)
		Ga[c]	
Sn	0.61133 (8)	0.28 (1)	1.005 (3)
Zr1	$^1/_3$	0.46 (2)	1
Zr2	0.2634 (1)	0.15 (2)	1.008 (3)
Z	0	0.42 (3)	0.840 (5)

[a] Atomic position types: Sn: x, 0, $^1/_4$; Zr1: $^1/_3$, $^2/_3$, 0; Zr2: x, 0, $^1/_4$; Z: 0, 0, 0. Only the x parameters are listed. [b] Rietveld refinement. [c] Nonstoichiometric phases from arc-melting; R/R_w = 4.2/6.3 and 2.7/3.7%, respectively.

The other compounds that contain the neighboring Ga and Ge show much different trends and provide us some basis for the interpretation of lattice dimension data for other Zr_5Sn_3Z phases. The Zr2–centroid distances in the antiprisms increase 0.21–0.24 Å from that of the empty host with these larger interstitials. The expanded Zr_6Z units now exhibit shortened Zr2–Sn interactions at the distinct expense of the longer Zr1–Sn bonds, again a matrix-like response. The net effect is the expansion of Zr2 clusters and a leveling off of the Zr–Sn distances of different types. These are presumably strong Zr2–Z interactions based on a general shortening of Zr2–Z bonds in not only Zr_5Sb_3Z[8] and Zr_5Pb_3Z[25] but also in centered zirconium cluster halides.[5] Comparative examples of sufficient accuracy are difficult to find for Zr–Ga and Zr–Ge distances. However, the Zr–Ga value, 2.74 Å, is distinctly less than 2.93 Å in Zr_2Ga ($CuAl_2$),[26] perhaps because of the more anisotropic, mixed environment about zirconium in the ternary. The average Zr–Ge distance in $ZrGe_2$, 2.87 Å (CN4,6; $ZrSi_2$ type),[27] compares with 2.78 Å in Zr_5Sn_3Ge.

The apparently intact and stoichiometric Zr_5Sn_3 part in all of the structures, even in the arc-melted samples, is quite remarkable (Table IV). This seems to be a noted contrast with the more ready substitution for Sb by Si or Al in those Zr_5Sb_3Z systems at high temperatures.[8]

(21) For $Zr_5Sn_3Sn_{0.096(6)}$, x = 0.6087 (1), 0.2480 (2) for Sn1, Zr2, respectively; R/R_w = 2.1/4.9%.
(22) Stuart, H.; Ridley, N. *J. Iron Steel Inst.* **1970**, *208*, 1087.
(23) Zainulin, Y. G.; Alyamovskii, S. I.; Shveikin, G. P.; Gel'd, P. V. *Inorg. Mater.* **1970**, *6*, 1192.
(24) Zhang, J.; Ziebarth, R. P.; Corbett, J. D. *Inorg. Chem.* **1992**, *31*, 614.
(25) Kwon, Y.-U.; Corbett, J. D. *J. Alloys Compounds*, in press.
(26) Havinga, F. E.; Damsma, H.; Hokkeling, P. *J. Less-Common Met.* **1972**, *27*, 169.
(27) Smith, J. F.; Bailey, D. M. *Acta Crystallogr.* **1957**, *10*, 341.

Table V. Important Distances in Some Zr_5Sn_3Z Phases (Å)

bond type	Z						
	empty[a]	$Sn_{0.10}$[b]	$Sn_{0.18}$[c]	C	O	Ga[d]	Ge
Zr2–Z	2.536	2.551 (1)	2.592 (1)	2.459 (1)	2.4562 (8)	2.743 (4)	2.775 (3)
Zr2–Sn							
interchain	3.068	3.058 (2)	3.035 (1)	3.102 (2)	3.093 (1)	2.982 (6)	2.939 (5)
out-of-plane	3.142	3.1413 (6)	3.139 (1)	3.1973 (8)	3.1875 (6)	3.121 (2)	3.104 (2)
in-plane	2.903	2.9076 (7)	2.918 (0)	2.9142 (9)	2.9190 (5)	2.980 (3)	2.977 (4)
Zr1–Sn	2.984	2.9895 (3)	3.001 (0)	2.9641 (3)	2.9582 (2)	3.057 (1)	3.054 (3)
Zr2–Zr2							
out-of-plane	3.565	3.580 (2)	3.615 (1)	3.443 (2)	3.445 (2)	3.743 (3)	3.767 (3)
in-plane	3.614	3.646 (3)	3.716 (1)	3.5118 (7)	3.5017 (6)	4.011 (8)	4.076 (6)
Zr1–Zr2	3.566	3.560 (3)	3.547 (1)	3.605 (1)	3.6004 (6)	3.531 (3)	3.500 (4)

[a] Extrapolated from data for $Zr_5Sn_3Sn_{0.10}$ and $Zr_5Sn_3Sn_{0.18}$. [b] Reference 21. [c] Reference 11. [d] Rietveld refinement.

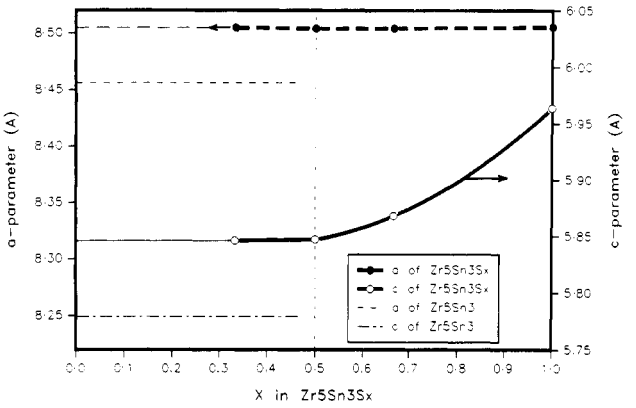

Figure 2. Unit cell parameters a (upper) and c (lower) for $Zr_5Sn_3S_x$ samples, $x = 0, {}^1/_3, {}^1/_2, {}^2/_3$, and 1.0. A biphasic system exists at 1050 °C for $0 < x < \sim{}^1/_2$.

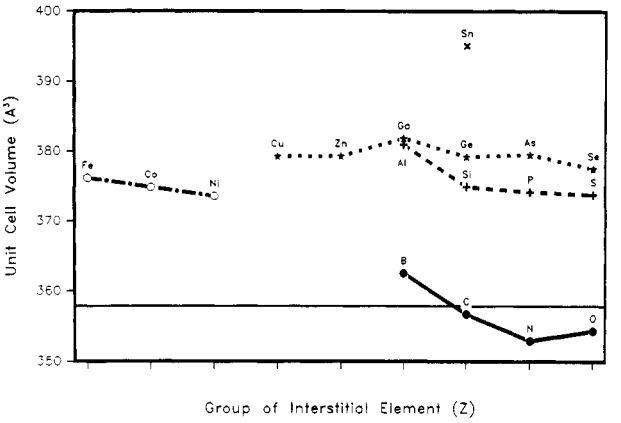

Figure 3. Unit cell volumes Zr_5Sn_3Z as a function of group and period of the interstitial element Z. ●, +, ★, × represent second-, third-, fourth-, and fifth-period elements, respectively. The Fe, Co, Ni data (open circles) are for $Zr_5Sn_3(Sn_{1/3}Z_{1/3})$ compositions (see text).

The lattice parameter variations with sulfur content in $Zr_5Sn_3S_x$, Figure 2, provide an interesting microscopic insights into substoichiometric interstitial systems and interatomic interactions. The powder patterns reveal a solid solution for $\sim{}^1/_2 < x < 1$, with no evidence of an ordered superstructure. Below this limit, there are two phases, $Zr_5Sn_3S_{\sim 1/2}$ and $Zr_5Sn_3S_{\sim 0}$. Although the latter must have a finite sulfur concentration, the result cannot be distinguished from the binary Zr_5Sn_3 by line positions. The invariant a parameter with varying sulfur content implies a fixed lateral dimension around the disordered interstitial atoms. On the other hand, the c length smoothly relaxes with decreasing concentration. The 0.5 sulfur limit can be viewed as the minimum concentration necessary to maintain the expanded a dimension, below which the strains of microscopically different portions of Zr_5Sn_3 and Zr_5Sn_3S cause a breakdown. The relatively rapid parabolic decrease in c with decreasing x is consistent with the marked relief of repulsions between neighboring interstitials rather than a macroscopic average of filled and empty units.

A unique feature of the sulfur system was that hkl reflections in the powder pattern with $l \neq 0$ were diffuse while those with $l = 0$ were fairly sharp over the nonstoichiometric region. This is characteristic of many disordered systems, reflecting a distribution of domains with different S–S separations and c parameters. On the basis of synthetic results for the stoichiometric limit, there is no reason to believe these solutions were not fully equilibrated. A superstructure with an ordered one-third occupancy is found for $La_5Ge_3Z_{1/3}$, Z = Mn, Fe, Co, Ni, Cu, C, O, P,[28] but this has not been seen in any of the zirconium systems studied.

The question of a significant substoichiometry with other Z has not been investigated very thoroughly. Samples of $Zr_5Sn_3Z_{1/2}$ for Z = Cu, Ga, Ge, As produced in the same way as before typically gave no clear phase separation, rather very broad lines, each of which basically spanned the region between those for the empty and full lattices. The behavior is not understood; perhaps temperatures >1000 °C are necessary for good growth of mixed crystals. Some evidence for substoichiometric behavior was noted with $Zr_5Sn_3O_x$ and is also known for $Zr_5Sb_3Sb_x$, $0 \leq x < 0.4$.[8] Notwithstanding, most ternaries in these two host systems and in La_5Ge_3 can certainly be obtained fully stoichiometric at 1000–1100 °C.

Unit cell volumes for Zr_5Sn_3Z as a function of the group and period of the Z atoms are presented in Figure 3. (The data plotted for Fe, Co, Ni are for the $Zr_5Sn_3(Sn_{1/3}Z_{1/3})$ compositions described above.) The overall behavior of these follow trends in metallic radii of the interstitial elements (covalent radii for the nonmetals)[29] quite well, with the largest expansion in each period at the boron group. Of course, cell volumes also reflect changes in four types of Zr–Sn distances, but the intrinsic volume properties of Z are still apparent. The fairly regular volume behavior shown for the sulfur and selenium derivatives contrasts with the sizable expansions found for the Zr_5Sb_3 counterparts.[8] On the other hand, the c/a ratios do show sizable increases for both Zr_5Sn_3S and Zr_5Sn_3Se, Figure 4. These deviations all appear to derive from repulsions between the relatively higher charged (more ionic) chalcogenides along a fairly short repeat along c ($c/2 \sim 2.98$ Å), with the pnictides next in magnitude of the effect. The

(28) Guloy, A. M.; Corbett, J. D., to be published.

(29) Pauling, L. *The Nature of the Chemical Bond*, 3rd ed.; Cornell University Press: Ithaca, NY, 1960; p 403.

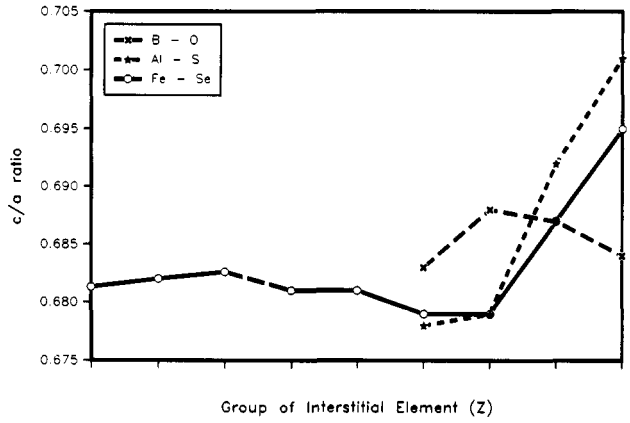

Figure 4. c/a ratios for Zr_5Sn_3Z phases as a function of group and period of the interstitial Z. ×, ★, ○ designate second-, third-, and fourth-period Z members, respectively. The first three in the last series refer to $Zr_5Sn_3(Sn_{1/3}Z_{1/3})$ compositions, Z = Fe, Co, Ni.

differences between these two Zr_5Sb_3Z and Zr_5Sn_3Z derive from the somewhat greater compensating contractions of the a parameter with tin that obscure the change in c on a volume basis.

Comparisons with Other Zr_5B_3Z Systems. Quite similar ranges of interstitial elements can be incorporated in Zr_5Sb_3Z,[8] Zr_5Sn_3Z, and Zr_5Pb_3Z[26] systems, all of which have in common the formation of local Zr_6Z units. The influence of the Sb, Sn, Pb components appear to be secondary and very minor. It must be remembered that the stabilities of alternate products are always the prime factor in the achievement of ternary examples or not; thus Zr_nZ alternative phases might be the common feature in the three types of zirconium systems. Complications with Fe, Co, Ni in Zr_5Sb_3 and Zr_5Sn_3 are similar, including fractional mixed interstitials and the intrusion of W_5Si_3-like ternaries when the amount of Sn or Sb is reduced.[10] Differences in the number of conduction electrons (n) in the hosts (8 for Zr_5Sn_3 and Zr_5Pb_3; 11 in Zr_5Sb_3) and in their analogous ternary products seem to afford no obvious differences in product stabilities. On the other hand, distinct differences are found in interstitial chemistry of the larger and electron poorer La_5Ge_3 and La_5Pb_3 (n = 3).[28]

Differences in lattice parameter variations between some Zr_5Sb_3Z and Zr_5Sn_3Z products are quite striking. The Zr_5Sb_3Z phases exhibit a much greater cell contraction with second period C and O, >12 Å^3, while the Zr_5Sn_3Z analogues change by only 1.2 and 3.6 Å^3. Other groups of interstitials show, overall, closer values of cell volume increases. The smaller size of Sb and, in turn, the smaller unit cell of Zr_5Sb_3Z appears to be the major reason for the differences with light Z. The polarities of Zr–Sb vs Zr–Sn in the hosts may also be a factor; this point is supported by the more similar unit cell volume changes found for the Zr_5Pb_3Z[25] and Zr_5Sn_3Z systems even though the host in the former is much larger and probably more flexible.

The term "Nowotny phase" was invented to define compounds that were thought to be stable in this structure type only when they included bound interstitials.[30] While many of the examples originally proposed in fact do not so behave, the lack of high-purity reagents, good containers, furnaces, etc., at that time precluded critical evaluations. However, we do find that a Zr_5In_3Z series in Mn_5Si_3-type structure are stable for Z = Cu, Al, ..., while no Zr_5In_3 phase is known.[31] The same is true of La_5Sn_3O in this structure[32] and, in a different sense, for $La_5Pb_3(O,N)$ in a Cr_5B_3-like structure whereas La_5Pb_3 is Mn_5Si_3-type.[33] The role of mixed and even partial interstitials should also not be underestimated.

These broad ranges of interstitial compounds in a common structure type obviously offer new and attractive means for tuning properties.

Acknowledgment. The oxide crystal was synthesized and the structure first refined by Ed Garcia. The authors are indebted to H. F. Franzen, K. Gschneider, R. A. Jacobson, and L. Daniels for the continued provision of arc-melting, induction heating, Ta welding, and diffractometer facilities and to S. Sevov for the SEM examinations.

Supplementary Material Available: Additional data collection and anisotropic displacement parameter information for Zr_5Sn_3Z, Z = C, O, Ge (2 pages); structure factor data for the same compounds (5 pages). Ordering information is given on any current masthead page.

(30) Kieffer, R.; Benesovsky, R.; Lux, B. *Planseeber.* **1956**, *5*, 30.
(31) Kwon, Y.-U.; Bularzik, J.; Corbett, J. D., unpublished research.
(32) Kwon, Y.-U.; Rzeznik, M.; Guloy, A.; Corbett, J. D. *Chem. Mater.* **1990**, *2*, 546.
(33) Guloy, A. M.; Corbett, J. D. *Z. Anorg. Allg. Chem.*, in press.